

Variable Coefficient of Friction: An effective VFPI parameter to control near-fault ground motion

Girish Malu¹ and Pranesh Murnal²

1. Research Scholar, Shivaji University, Kolhapur, India and Associate Professor, Dr. J. J. Magdum College of Engineering, Jaysingpur, India

2. Professor, Department of Applied Mechanics, Government College of Engineering, Aurangabad, India

ABSTRACT: Several sliding isolation systems have been proposed to control earthquake effects. However most of these isolation devices have limited effectiveness under near-fault ground motions due to pulse-type characteristics of such excitations. Recently proposed, VFPI has unique characteristics to overcome the limitations of traditional isolation system for near-fault ground motions. VFPI incorporates isolation, energy dissipation and restoring force mechanisms and has additional advantages due to response-dependent variable frequency of oscillation and bounded restoring force. The device has wide choice of parameters to choose from, as per design requirements. In this paper, behaviour of single storey structures isolated using VFPI subjected to near-fault ground motions have been numerically examined. It is shown that it is possible to increase effectiveness of VFPI by using discretely varying coefficient of friction along sliding surface. Parametric studies have been carried out to critically examine the behaviour of single storey structures isolated with VFPI and FPS system.

KEY WORDS: Base isolation, VFPI, Near-fault ground motions, Passive control.

INTRODUCTION

Base isolation has emerged as an effective technique in minimizing the earthquake forces. In this technique, a flexible layer (or isolator) is placed between the super structure and its foundation such that relative deformations are permitted at this level. Due to flexibility of the isolator layer, the time period of motion of the isolator is relatively long; as a result the isolator time period controls the fundamental period of the isolated structure. For properly designed isolation system, the isolator time period is much longer than those containing significant ground motion energy. As a result, use of isolator shifts the fundamental period of the structure away from the predominant periods of ground excitation. Extensive review of base isolation systems and its applicability is available in literature (Buckle and Mayes, 1990; Kelly, 1993; Naeim and Kelly, 1999).

Practical isolation devices typically also include energy dissipating mechanism so as to reduce deformations at the isolator level. For example friction type base isolators, uses a sliding surface for both isolation and energy dissipation, and has been found to be very effective in reducing structural response (Mostaghel et al., 1983). Due to the characteristics of excitation transmitted through sliding surface, the performance of friction isolators is relatively insensitive to severe variations in the frequency content and amplitude of the input excitation, making performance of sliding isolators very robust. The simplest sliding isolator consists of horizontal sliding surface (Pure-Friction or PF system), which may experience large sliding and residual displacements, and are often difficult to incorporate in structural design.

To overcome the difficulty of restoring force an effective mechanism to provide restoring force by gravity has been utilised in Friction Pendulum System (FPS) (Zayas et al., 1987). In this system, the

sliding surface takes a concave spherical shape so that the sliding and re-centring mechanisms are integrated in one unit. The FPS isolator has several advantages over PF system, and has demonstrated acceptable performance for many different structures and excitation characteristics (Mokha et. al., 1991, 1996; Tsopelas et. al., 1996; Tsai, 1997; Wang et. al., 1998). Apart from advantages of FPS the main disadvantage of FPS is that it has a constant time period of oscillation due to its spherical surface. As a result FPS isolators can be effectively designed for a specific level (amplitude and frequency characteristics) of ground excitation. Under more severe ground motions, sliding displacement greater than design displacement can occur, which may lead to very large accelerations and failure of FPS isolator. Since in FPS isolator, restoring force is linearly proportional to sliding displacement, the large amount of sliding introduces significant additional energy in the structure. As a result, the maximum intensity of excitation has a strong influence on FPS design. In general, FPS isolator designed for particular level of excitation may not give satisfactory performance during earthquake with much lower or higher intensity (Sinha and Pranesh, 1998). Due to constant value of frequency a resonant problem may occur when the structure resting on FPS is subjected to a ground motion of a frequency close to the isolation frequency (Krishnamoorthy, 2010).

Due to the limitations of FPS, many researchers have tried different geometries for the sliding surface of the isolator. A recently developed new isolator called the Variable Frequency Pendulum Isolator (VFPI) incorporates the advantages of both the FPS and PF isolators and overrules disadvantages of FPS and PF isolators (Pranesh and Sinha, 1998; Pranesh, 2000). Probably this is the first attempt to propose the concept of variable frequency in sliding type isolators, although concept of variable curvature is found in literature earlier (Sustov, 1992). Lu et. al., (2006) generalised the mathematical formulation of a sliding surface with variable curvature using a polynomial function to define the geometry of the sliding surface. In this paper experimental and analytical study of performance of three sliding type isolators (including VFPI) has been carried out. Krishnamoorthy (2010) also proposed a sliding surface with variable frequency and variable friction coefficient. Krishnamoorthy proposed the isolator having radius of curvature varying exponentially with sliding displacement and friction coefficient also varying with sliding displacement. However VFPI is found to be more effective under variety of excitations and structures because of the following properties of VFPI: (1) its time period of oscillation depends on sliding displacement, and (2) its restoring force has a bounded value and exhibits softening behaviour for large displacements (Malu and Pranesh, 2010). The geometry of sliding surface has been defined by second order parametric equation. As a result, the isolator properties can be chosen to achieve progressive period shift with variation in sliding displacement. These properties can be controlled by a set of VFPI parameters, which is otherwise not possible in single parameter systems like FPS.

The study of structures subjected to near-fault ground motions has a special significance due to the nature of such ground motions. Near-fault ground motions are characterised by pulse type excitations having narrow range of relatively lower frequencies. Near-fault ground motions often contain strong coherent dynamic long period pulses and permanent ground displacements. The dynamic motions are dominated by large long period pulses of motions that occur on the horizontal component perpendicular to strike of fault, caused by rupture directivity effects. This pulse is narrow band pulse which causes the response spectrum to have a peak, such that the response due to near-fault ground motions of moderate magnitude may exceed those of large magnitude at intermediate periods. The radiation pattern of the shear dislocation on the fault causes this large pulse of motion to be oriented in the direction perpendicular to fault plane, causing the strike-normal component of ground motion to be larger than the strike-parallel component. The strike-parallel motion causes permanent ground displacement (fling step) whereas the strike-normal component causes significantly higher dynamic motion (Somerville, 1997, 2005).

Structures isolated by most base isolation devices have a long time period which is fairly constant. Since the near fault ground motions have a long period pulse type motions they induce very large displacements at the isolation level. As a result base isolated structures do not perform well under near-fault ground motions. But it has been demonstrated that the newly developed isolator VFPI can be effective under both near-fault and far-field ground motions if proper VFPI parameters are adopted in the design (Murnal and Malu, 2007; Malu and Murnal, 2010). However it is difficult to control the large sliding displacements that could occur during near-fault ground motions.

In the present paper it is proposed to change the coefficient of friction at predefined location along the VFPI isolator surface so that sliding displacement can be controlled under near field ground motion. A smaller value of coefficient of friction for smaller sliding displacement and a larger value for larger sliding displacement is likely to control the displacement due to higher energy dissipation due to increased friction force. The effectiveness of VFPI with discretely variable coefficient of friction is examined through a parametric study on SDOF models (2-DOF models when isolated) subjected to near-fault ground motions.

VFPI DESCRIPTION

1. Mathematical preliminaries

Consider the motion of a rigid block of mass m sliding on a smooth curved surface of defined geometry, $y = f(x)$. The restoring force offered by curved sliding surface can be defined as the lateral force required to cause the horizontal displacement, x . Assuming point contact the various forces acting on sliding surface when the block is displaced from its original position at the origin of coordinate axes are as shown in Figure 1. At any instant the horizontal restoring force due to weight of the structure is given by

$$f_R = mg \frac{dy}{dx} \quad (1)$$

Assuming that the restoring force is mathematically represented by an equivalent non-linear mass-less horizontal spring, the spring force can be expressed as the product of the equivalent spring stiffness and the deformation, i.e.,

$$f_R = k(x)x \quad (2)$$

where, $k(x)$ is the instantaneous spring stiffness, and x is the sliding displacement of the mass.

If the mass is modelled as a single-degree-of-freedom oscillator, the spring force (restoring force) can be expressed as the product of the total mass of the system and square of oscillation frequency

$$f_R = m\omega_b^2(x)x \quad (3)$$

Here, $\omega_b(x)$ is the instantaneous isolator frequency, and depends solely on the geometry of sliding surface. In Friction Pendulum System, which has a spherical sliding surface, this frequency is almost constant and is approximately equal to $\sqrt{g/R}$, where R is the radius of curvature of the sliding surface (Zayas et al., 1990).

2. Variable frequency pendulum isolator geometry

Sliding surface based on the expression of an ellipse has been used as the basis for developing sliding surface of VFPI (Pranesh, 2000). The equation of an ellipse with a and b as its semi-major and semi-minor axes, respectively, and with co-ordinate axes as shown in Figure 1 is given by,

$$y = b(1 - \sqrt{1 - x^2/a^2}) \quad (4)$$

Differentiating with respect to x , the slope at any point on the curve is given by

$$\frac{dy}{dx} = \frac{b}{a^2 \sqrt{1 - x^2/a^2}} x \quad (5)$$

If the equation of sliding surface is represented by Equation (4), the frequency of oscillation can be determined by substituting Equation (5) in Equations (1) and (3). As a result expression for frequency of elliptical surface is given by

$$\omega_b^2(x) = \omega_I^2 / \sqrt{1 - x^2/a^2} \quad (6)$$

where, $\omega_I^2 = gb/a^2$ = square of initial frequency of isolator (at zero sliding displacement).

It can be seen that the frequency of an elliptical curve is fairly constant for small displacements ($x \ll a$) and this value depends upon the ratio b/a^2 . From this expression it is observed that the frequency of the surface is inversely proportional to the square of semi-major axis and an increase in its value results in sharp decrease in the isolator frequency. So to get the desired variation of the frequency, the semi-major axis of the ellipse, a , has been taken as a linear function of sliding displacement x and is expressed as a variable in getting the geometry of VFPI. The semi-major axis can be expressed as

$$a = x + d \quad (7)$$

where, d is a constant. Substituting in Equation (4), the expression for geometry of sliding surface of VFPI is expressed as

$$y = b \left[1 - \frac{\sqrt{d^2 + 2d x \operatorname{sgn}(x)}}{d + x \operatorname{sgn}(x)} \right] \quad (8)$$

where, $\operatorname{sgn}(x)$ is the signum function introduced for maintaining symmetry of sliding surface about the central vertical axis. This assumes a value of +1 for positive sliding displacement and -1 for negative sliding displacement. It is observed from Equation (8) that the upper bound of vertical displacement is equal to b , and it occurs only at infinitely large horizontal displacement. The slope at any point on this sliding surface is given as

$$\frac{dy}{dx} = \frac{bd}{(d + x \operatorname{sgn}(x))^2 \sqrt{d^2 + 2dx \operatorname{sgn}(x)}} x \quad (9)$$

To simplify the notations, a non-dimensional parameter $r = x \operatorname{sgn}(x)/d$ is used. By substituting r and the initial frequency $\omega_I^2 = gb/d^2$ in Equation (9), and combining with Equations (1) and (2), the isolator frequency at any sliding displacement can be expressed as

$$\omega_b^2(x) = \frac{\omega_I^2}{(1+r)^2 \sqrt{1+2r}} \quad (10)$$

In the above equations, parameters b and d completely define the isolator characteristics. It can be observed that the ratio b/d^2 governs the initial frequency of the isolator. Similarly, the value of $1/d$ determines the rate of variation of isolator frequency, and this factor has been defined as

frequency variation factor (FVF). It can also be seen from Equation (10) that the rate of decrease of isolator frequency is directly proportional to FVF for given initial frequency. The variation of oscillation frequency of a typical VFPI with respect to the sliding displacement is shown in Figure 2(a). For comparison purposes, the oscillation frequency of FPS with same initial frequency has also been shown, which is found to be almost constant. From this plot it is seen that the oscillation frequency of VFPI sharply decreases with increasing sliding displacement and asymptotically approaches zero.

The force-deformation hysteresis obtained from Equation (3), for a typical FPS and VFPI, are shown in Figure 2(b). In this plot, the isolator force (restoring force + frictional force) has been normalised with respect to mg and the both constant and discretely variable coefficient of friction are considered. It can be observed that the isolator force in VFPI first increases to reach its maximum value, and later slowly decreases so as to asymptotically approach the frictional force at large sliding displacement for constant coefficient of friction. This is an important property of VFPI, which limits the force transmitted to the structure. Beyond the peak restoring force the VFPI does not lose the restoring capability as a small amount of restoring force is always available. It is also observed that for very small displacements variation in restoring force is approximately linear. In the FPS, on the other hand, the restoring force always increases linearly with the sliding displacement. From this it can be concluded that, behaviour of VFPI, is similar to FPS for small displacements and similar to PF for large displacements without significant loss of restoring capability. In case of variable coefficient of friction isolator force suddenly changes at a point where coefficient of friction value has been changed, and rest of the variation remaining same. This will change the energy dissipation characteristics of the isolator which may help in controlling the sliding displacements.

The geometry of sliding surface of VFPI and FPS are as shown in Figure 3. From Figure 3 it can be easily observed that the VFPI is flatter than FPS, which results in smaller vertical displacement for similar sliding displacement in the structure and hence may lead to smaller overturning moment.

MATHEMATICAL FORMULATION

Consider a single storey shear structure isolated by sliding type isolator (two DOF system when isolated) subjected to a horizontal ground excitation \ddot{x}_g (Figure 4). Figure 1 shows the forces acting on isolator when sliding is in positive x direction.

1. Equations of motion

The motion of structure can be in either of the two phases: non-sliding phase and sliding phase. In non-sliding phase, the structure behaves like a conventional fixed base structure since there is no relative motion at the isolator level. When the frictional force at the sliding surface is overcome, there is a relative motion at the sliding surface, and the structure enters sliding phase. The total motion consists of a series of alternating non-sliding and sliding phases in succession.

2. Non-sliding phase

In non-sliding phase the structure behaves as a fixed-base structure. There is no relative motion between the ground and base mass since the static frictional resistance is greater than the horizontal force acting on the structure. The Equations of motion in this phase are:

$$\ddot{x}_r + 2\xi_o\omega_o\dot{x}_r + \omega_o^2x_r = -\ddot{x}_g \quad (11)$$

and

$$x_b = \text{constant}; \dot{x}_b = \ddot{x}_b = 0 \quad (12)$$

where, x_r is the relative displacement of the top mass with respect to the base mass, x_b is the displacement of the base mass (m_b) relative to the ground, x_g is the ground displacement. Over-dot indicates derivative with respect to time, $\omega_o = \sqrt{k_o/m}$ and $\xi_o = c_o/2\sqrt{k_o m}$ are the frequency and damping ratio respectively of the fixed base SDOF structure. Before application of ground motion the structure is at rest, as a result the motion of structure always starts in non sliding phase. The structure is classically damped in this phase and hence equation of motion can be readily solved by usual modal analysis procedures (Clough and Penziene, 1993).

3. Initiation of sliding phase

When the structure is subjected to base excitation, it will remain in non-sliding phase unless the frictional resistance at the sliding surface is overcome. It means the absolute value of sum of the total inertia force and restoring force should be greater than or equal to the absolute value of frictional force acting along the sliding surface. The frictional force depends on the coefficient of friction at the location at given instant. The plan of a typical isolator with two discrete values of coefficient of friction considered in this study is shown in Figure 5. The coefficient of friction μ_1 is assumed to be less than μ_2 in this study. Therefore the condition for the beginning of sliding phase can be written as,

$$\left| \left[m(\ddot{x}_r + \ddot{x}_g) + m_b \ddot{x}_g \right] \cos \theta + (m + m_b)g \sin \theta \right| \geq \mu(m + m_b)g \cos \theta \quad (13)$$

where, θ is the angle of tangent at the point of contact with horizontal and $\mu = \mu_1$ or μ_2 , is the coefficient of friction at respective isolator position. Now dividing Equation (13) by $\cos \theta$ and substituting dy/dx_b for $\tan \theta$ the condition for sliding can be simplified as,

$$\left| \left[m(\ddot{x}_r + \ddot{x}_g) + m_b \ddot{x}_g \right] + (m + m_b)g \frac{dy}{dx_b} \right| \geq \mu(m + m_b)g, \mu = \mu_1 \text{ or } \mu_2 \quad (14)$$

$(m + m_b)g \frac{dy}{dx_b}$ is the restoring force [Equation (1)]. If it is expressed as a product of spring stiffness and sliding displacement, the spring force is given by [Equation (3)],

$$f_R = (m + m_b)\omega_b^2(x_b)x_b \quad (15)$$

where, $\omega_b(x_b)$ is the isolator frequency at the any instant of sliding displacement x_b . Dividing Equation (14) by the total mass and defining the mass ratio as,

$$\alpha = \frac{m}{m + m_b} \quad (16)$$

The condition for initiation of sliding phase can be simply expressed as,

$$\left| \alpha \ddot{x}_r + \ddot{x}_g + \omega_b^2(x_b)x_b \right| \geq \mu g, \mu = \mu_1 \text{ or } \mu_2 \quad (17)$$

4. Sliding phase

Once the inequality [Equation (14)] is satisfied, the static frictional force is overcome, the structure enters sliding phase and the degree of freedom (DOF) corresponding to the base mass also experiences motion. During this phase, the structure behaves like a two-degree-of-freedom structure. The equations of motion for top and bottom mass are, respectively given by

$$\ddot{x}_r + 2\xi_o \omega_o \dot{x}_r + \omega_o^2 x_r = -\ddot{x}_b - \ddot{x}_g \quad (18)$$

and

$$\alpha \ddot{x}_r + \ddot{x}_b + \omega_b^2(x_b) x_b = -\ddot{x}_g - \mu g \operatorname{sgn}(\dot{x}_b), \quad \mu = \mu_1 \text{ or } \mu_2 \quad (19)$$

5. End of sliding phase

A sliding phase ends when the sliding velocity of base mass becomes equal to zero, i.e.

$$\dot{x}_b = 0 \quad (20)$$

As soon as this condition is satisfied, Equations (11) and (12) corresponding to non sliding phase need to be evaluated to further check the validity of the inequality in Equation (17). This decides whether the structure continues in the sliding phase after a momentary stop or enters in a non-sliding phase.

6. Direction of sliding

Once inequality [Equation (17)] is satisfied, the structure starts sliding in a direction opposite to the direction of the sum of total inertia force and restoring force at the isolator level. So, the direction of sliding can be decided based on the signum function as defined below.

$$\operatorname{sgn}(\dot{x}_b) = -\frac{\alpha \dot{x}_r + \ddot{x}_g + \omega_b^2(x_b)}{|\alpha \dot{x}_r + \ddot{x}_g + \omega_b^2(x_b)|} \quad (21)$$

The signum function remains unchanged in a particular sliding phase until the sliding velocity of the base mass becomes equal to zero. Once the sliding velocity is zero, the structure may enter a non-sliding phase, reverse its direction of sliding, or have a momentary stop and then continue in the same direction. To determine the correct state, the solution process needs to continue using equations of non-sliding phase wherein the sliding acceleration is forced to zero and the validity of the inequality [Equation (17)] is checked. If this inequality is satisfied at the same instant of time when the sliding velocity is zero, then Equation (21) decides the further direction of sliding.

RESPONSE OF AN EXAMPLE SYSTEM

The effectiveness of VFPI with variable coefficient of friction to reduce response of an example single storey structure subjected to near-fault earthquake excitations has been presented in this section. The example structure, under fixed base condition is represented as a single-degree-of-freedom (SDOF) system with value of spring stiffness and lumped mass so that the period of structure is 0.5 s. The mass of structure and base are taken equal, so that the mass ratio, $\alpha = 0.5$.

Narasimhan and Nagarajaiah (2006) have proposed a variable friction system to adjust the level of friction in the base isolated structure. Panchal and Jangid (2008) proposed a sliding surface by varying the friction coefficient along the sliding surface in the form of curve of FPS and called isolator as VFPS (Variable Friction Pendulum Isolator). In this case the value of coefficient of friction is changing from minimum of 0.025 to maximum of 0.15 and then again reduces and approaches nearly to 0.015. Krishnamoorthy (2010) proposed Variable Frequency and Variable Friction Pendulum Isolator (VFFPI). Here the value of coefficient of friction is changing from a minimum of 0.08 to a maximum of 0.1 from 0.0 m to 0.18 m from the centre of the sliding surface. These studies show that a sliding isolator with either a varying radius of curvature or a varying friction coefficient may be used as an effective isolator for isolating the structure. Most of these studies have focussed on the effectiveness of the isolator in reducing accelerations under different excitations. All these isolators are likely to be of limited effectiveness under near-fault ground motions due to very high sliding displacements. Further, practically a sliding surface with a continuously variable coefficient of friction of desired variation may be difficult to achieve. Hence in the present study performance of VFPI with

two discrete values of coefficients of friction under near-fault ground motion has been carried out (initial coefficient of friction (μ_1) and final coefficient of friction (μ_2)).

The behaviour has been studied through time history analysis for ten near-fault ground motions. The details of the ground motions used in the study are presented in Table 1. These ground motions are derived from historical recordings. The ground motions chosen cover a wide variety of near-fault ground motions having different peak ground acceleration (PGA), frequency composition and duration. For a given coefficient/s of friction, the main parameters of VFPI affecting the response are (i) initial time period and (ii) Frequency Variation Factor (FVF). For the present analysis FVF has been varied from 1.0 per m to 10.0 per m for VFPI with two values of initial time period, 1 s and 2 s. To investigate the effectiveness of VFPI, the responses are compared with those of structure isolated using FPS with isolator period equal to 2.0 s, since $T = 2$ s is a practical value of time period for FPS.

To study the effect of variable coefficient of friction on the behaviour of VFPI-isolated structure two values of coefficients of friction considered are $\mu_1 = 0.05$ and $\mu_2 = 0.1$. VFPI with these two constant coefficients of friction are first analysed separately and then they are combined in the same isolator, the latter case being referred to as variable coefficient of friction case. In variable coefficient of friction case initial coefficient of friction (μ_1) refers to the coefficient of friction up to a pre-defined distance from the centre of the isolator (d_b) and the coefficient of friction beyond this distance is referred to as final coefficient of friction (μ_2). In the present study the initial coefficient of friction (μ_1) is considered as 0.05 and final coefficient of friction (μ_2) as 0.1. This will enable larger energy dissipation for larger sliding displacement which may help to control the sliding displacements. Three positions of change of coefficient of friction (d_b) are considered here namely, 0.1 m, 0.2 m and 0.3 m from the centre of the isolator. The structural damping is assumed as 5% of critical.

1. Time history response

The response quantities are evaluated by solution of the equations of motion as discussed in the preceding sections. The main response quantities of interest are absolute acceleration of top storey and sliding displacement of isolator. To show the effectiveness of VFPI with respect to FPS typical time history graphs for NFR-01 (Tabas, 1978 normal component) are shown in Figures 6 and 7. Figure 6 shows the acceleration time history for VFPI and FPS with constant coefficient of friction of 0.05. As expected it is seen that the accelerations are substantially reduced in case of VFPI as compared to FPS.

It is expected that varying the coefficient of friction along the sliding surface will lead to decrease in sliding displacement which is usually a matter of concern for VFPI especially under near-field ground motions. To show the effectiveness of variable coefficient of friction typical time history graphs of sliding displacement under NFR-01 are shown in Figure 7. The figure shows the sliding displacement for constant coefficient of friction and variable coefficient of friction for different values of d_b . It is seen that the sliding displacements are effectively controlled with variable coefficient of friction and is more effective for lesser values of d_b . This means that it is possible to control the sliding displacements using variable coefficient of friction under near-field ground motions without significant increase in accelerations.

To further ascertain the effectiveness of variable coefficient of friction in reducing sliding displacements, force deformation history for NFR-01, VFPI ($T_i = 2$ s), $FVF = 2$, $d_b = 0.1$ m, is presented in Figure 8. From the figure it is clear that the sliding displacement is controlled in case of variable coefficient of friction due to higher energy dissipation in case of variable coefficient of friction as the area under force deformation graph increases due to the increased coefficient of friction at predefined point.

2. Effect of variable coefficient of friction

Under near-fault excitations, FPS may be able to control sliding displacements, but it may lead to very high level of structural accelerations due to long-period pulse type components in the excitation. On the other hand VFPI can control the accelerations but at the cost of high sliding displacements. So VFPI with variable coefficient of friction is likely to control both accelerations and sliding displacements. Varying the coefficient of friction may not help in case of FPS as the displacements are already controlled with constant coefficient of friction and accelerations are bound to be high in any case due to the constant time period of FPS. So to present the responses with effective comparison and comprehension the maximum response quantities of structures isolated with VFPI are normalised with respect to the corresponding response quantity of FPS having a constant time period of 2.0 s and the corresponding value of coefficient of friction. For example the maximum response values of VFPI with $\mu = 0.05$ are normalised with respect to maximum response value of FPS with $\mu = 0.05$ and maximum response values of VFPI with $\mu = 0.1$ are normalised with respect to maximum response value of FPS $\mu = 0.1$. In variable coefficient of friction case the response quantities have been normalised with FPS having a constant coefficient of friction of 0.05 as varying the coefficient of friction in case of FPS will not add to any advantage in the performance. It means the maximum response values of VFPI with variable coefficient of friction are normalised with respect to maximum response value of FPS $\mu = 0.05$. So the isolation is more effective when the normalised accelerations are less than unity (less than corresponding FPS response) and normalised sliding displacements are marginally greater than unity (displacement control equivalent to FPS).

For different cases under consideration, time history analyses have been carried out for all the ten near-fault ground motions indicated in Table 1. Since these earthquakes cover a wide variety of near-fault ground motion, the average of the maximum responses under the ten ground motions is considered for discussion. The average responses have been normalised with the average response of corresponding FPS isolated structure as explained earlier. The average FPS responses, using which average VFPI responses are normalised, are given in Table 2. The normalised peak accelerations and peak sliding displacements for different cases are represented in Figures 9 to 12

From Figures 9 and 10 it is observed that the accelerations are substantially reduced in case of VFPI when compared to those with FPS in all the cases as expected. When the initial time period of VFPI is 1.0 s, it is observed that the accelerations sharply decrease with FVF (because of sharp decrease in restoring force), whereas there is no significant decrease in the accelerations with FVF in case of VFPI with initial time period of 2.0 s. As expected the accelerations under a lower coefficient of friction of 0.05 are substantially lower than that with a higher coefficient of friction of 0.1. It is further observed that the accelerations are significantly lower in cases of variable coefficient of friction cases also. It is seen that accelerations in all variable coefficient of friction cases (with different values of d_b) fall between the accelerations for the two constant coefficients of friction cases. However they are more close to the lower bound of accelerations for case with coefficient of friction of 0.05, which shows the effectiveness of variable coefficient of friction in acceleration reduction.

From Figures 11 and 12 it is observed that the normalised sliding displacements increase with increase in FVF in all cases since increase in FVF leads to reduction in restoring force. As expected the displacements for lower coefficient of friction are higher than those with higher coefficient of friction. It is interesting to note that the sliding displacements in some variable coefficient of friction cases ($d_b=0.1m$) are lower than both cases of constant coefficient of friction. It is also seen that the sliding displacements are significantly lower for an FVF of 4 to 6 for VFPI with initial time period of 1.0 s and for an FVF of 1 to 3 for VFPI with initial time period of 2.0 s. It can be further confirmed that for this range of FVF the accelerations are also significantly lower (around 20 to 30 % of FPS case). So it

can be concluded that by varying the coefficient of friction at suitable location on the isolator surface and selecting a suitable FVF and initial time period, it is possible to control both accelerations and sliding displacements.

CONCLUSIONS

The effectiveness of a recently developed isolation system, Variable Frequency Pendulum Isolator (VFPI) for vibration control of single storey structure subjected to near-fault ground motions has been investigated in this paper. For effectiveness of VFPI for controlling both accelerations and sliding displacements under near field ground motions, variable coefficients of friction for the sliding surface has been proposed in this paper. Based on the investigations the following conclusions can be drawn.

1. The VFPI has a wide choice of parameters that can be chosen to suit the design requirements.
2. VFPI is very effective for acceleration reduction under the action of near-fault ground motions with corresponding increase in sliding displacements.
3. It is possible to control both accelerations and sliding displacements by using variable coefficient of friction and by choosing carefully the VFPI parameters.

References

1. Agrahara Krishnamoorthy, (2010). "Seismic isolation of bridges using variable frequency and variable friction pendulum isolator system", *Structural Engineering International*, Vol. 2, pp. 178-184.
2. Buckle, I.G. and Mayes, R.L. (1990). "Seismic isolation: history, application and performance - a world view", *Earthquake Spectra*, Vol. 6, No. 2, pp. 161-201.
3. Clough, R.W. and Penziene, J. (1993). "Dynamics of Structures", 2nd edition, McGraw-Hill, Inc., New York, USA.
4. Kelly, J.M. (1993). "State-of-the-art and state-of-the-practice in base isolation", Seminar on Seismic Isolation, Passive Energy Dissipation and Active Control (ATC-17-1), Applied Technology Council, Redwood City, CA, USA.
5. Lu, L.Y., et. al. (2006). "Sliding isolation using variable frequency bearing for near-fault ground motion", *Proceedings of the 4th International Conference on Earthquake Engineering*, Taipei, Taiwan.
6. Malu, G. and Murnal, P. (2010). "Behaviour of structure with VFPI during near-fault ground motion", *Proceedings of the International Conference on Innovative World of Structural Engineering*, Aurangabad, Vol. 1, pp. 166-174.
7. Mokha, A, et. al., (1990). "Teflon Bearings in Base Isolation I: Testing", *Journal of Structural Engineering*, Vol. 116, No. 2, pp. 438-454.
8. Mostaghel, N., et. al. (1983). "Response of sliding structures to harmonic support motion", *Journal of Earthquake Engineering and Structural Dynamics*, Vol. 11, No. 3, pp. 355-366.
9. Murnal, P. and Malu, G.M. (2007). "Selection of VFPI parameter for isolation effectiveness during near field ground motion", *Proceedings of the 8th Pacific conference on earthquake engineering*, Singapore, Paper No. 105
10. Naeim F. and Kelly J. M. (1993). "Design of seismic isolated structures: from theory to practice", John Wiley and Sons, New York, NY, USA.
11. Narasimhan, S. and Nagarajaiah, S. (2006). "Smart base isolated buildings with variable friction systems: H controller and SAIVF device", *Earthquake Engineering and Structural Dynamics*, Vol. 35, No. 8, pp. 921-942.

12. Panchal, V.R. and Jangid, R.S. (2008). "Variable friction pendulum system for seismic isolation of liquid storage tanks", Nuclear Engineering and Design, Vol. 238, pp. 1304-1315.
13. Pranesh, M. (2000). "VFPI: An innovative device for aseismic design", Ph.D. Dissertation, Indian Institute of Technology, Bombay, India.
14. Pranesh, M. and Sinha, R. (1998). "Vibration control of primary-secondary systems using variable frequency pendulum isolator", Proceedings of the 11th Symposium on Earthquake Engineering, Roorkee, pp. 697-704.
15. Pranesh, M., and Sinha, R. (2000). "VFPI: An isolation device for aseismic design", Journal of Earthquake Engineering and Structural Dynamics, Vol. 29, No. 5, pp. 603-627.
16. Sinha, R. and Pranesh, M. (1998). "FPS isolator for structural vibration control", Proceedings of the International Conference on Theoretical, Applied, Computational and Experimental Mechanics (CD Volume), IIT, Kharagpur, India
17. Somerville, P. (1997). "Engineering characteristics of near fault ground motion", Proceedings of the SMIP97 Seminar, pp. 9-28.
18. Somerville, P.G. (2005). "Engineering characterization of near fault ground motion", Proceedings of the 2005 New Zealand Society for Earthquake Engineering Conference, Paper No. 1, pp. 1-8.
19. Sustov, V. (1992). "Base isolation: Fresh insight", Proceedings of the 10th World Conference on Earthquake Engineering, Balkema, Rotterdam, pp. 1983-1986.
20. Tsai, C.S. (1997). "Finite element formulation for friction pendulum seismic isolation bearings", International Journal for Numerical Methods in Engineering, Vol. 40, pp. 29-49
21. Tsopelas, P., et. al. (1996). "Experimental study of FPS system in bridge seismic isolation", Journal of Earthquake Engineering and Structural Dynamics, Vol. 25, pp. 65-78.
22. Wang, Y.P., et. al. (1998). "Seismic response analysis of bridges isolated with friction pendulum bearings", Journal of Earthquake Engineering and Structural Dynamics, Vol. 27, pp. 1069-1093.
23. Zayas, V.A. et. al. (1987). "The FPS earthquake resisting system: Experimental report", Report No. UCB/EERC-87/01, Earthquake Engineering Research Centre, University of California, Berkeley, CA, USA
24. Zayas, V.A. et. al. (1990). "A simple pendulum technique for achieving seismic isolation", Earthquake Spectra, Vol. 6, No. 2, pp. 317-333.

List of Tables

Table 1	Details of earthquake records used in this study
Table 2	Average peak response values for FPS isolator used for normalization

List of Figures

Fig. 1	Free body diagram of sliding surface
Fig. 2	Properties of VFPI and FPS (constant $\mu=0.05$, variable $\mu_1=0.05$, $\mu_2=0.1$)
Fig. 3	Geometry of sliding surface of isolators: (a) PF (b) VFPI (c) FPS
Fig. 4	Analytical model of a single storey structure isolated by curved sliding surface
Fig. 5	Plan of typical isolator with variable coefficient of friction.
Fig. 6	Time history curve of storey acceleration for NFR-01, FVF = 2 (constant μ)
Fig. 7	Time history curve of sliding displacement for NFR-01, FVF = 2 (constant and variable μ)

- Fig. 8 Force deformation history of VFPI for constant and variable coefficient of friction for NFR-01, $FVF = 2$, $d_b = 0.1m$
- Fig. 9 Storey acceleration of VFPI ($T_i = 1s$) normalised w.r.t. peak value of FPS as in Table 2.
- Fig. 10 Storey acceleration of VFPI ($T_i = 2s$) normalised w.r.t. peak value of FPS as in Table 2.
- Fig. 11 Sliding displacement of VFPI ($T_i = 1s$) normalised w.r.t. peak value of FPS as in Table 2.
- Fig. 12 Sliding displacement of VFPI ($T_i = 2s$) normalised w.r.t. peak value of FPS as in Table 2.

Table 1 Details of earthquake records used in this study

Sr. No.	Name of earthquake	Designation	Magnitude	Distance of source (km)	PGA (g)	Duration (sec)
1	Tabas, 1978	NFR-01	7.4	1.2	0.900	50
2	Loma Prieta, 1989, Los Gatos	NFR-02	7.0	3.5	0.718	25
3	Loma Prieta, 1989, Lex. Dam	NFR-03	7.0	6.3	0.686	40
4	C. Mendocino, 1992, Petrolia	NFR-04	7.1	8.5	0.638	60
5	Erzincan, 1992	NFR-05	6.7	2.0	0.432	21
6	Landers, 1992	NFR-06	7.3	1.1	0.713	50
7	Nothridge, 1994, Rinaldi	NFR-07	6.7	7.5	0.890	15
8	Nothridge, 1994, Olive View	NFR-08	6.7	6.4	0.732	60
9	Kobe, 1995	NFR-09	6.9	3.4	1.088	60
10	Kobe, 1995, Takatori	NFR-10	6.9	4.3	0.786	40

Table 2 Average peak response values for structure isolated by FPS ($T = 2s$), used for normalization

Sr. No.	Description	Unit	Coefficient of friction	
			0.05	0.1
01	Storey Acceleration	m/s^2	12.915	8.140
02	Sliding Displacement	M	0.614	0.490

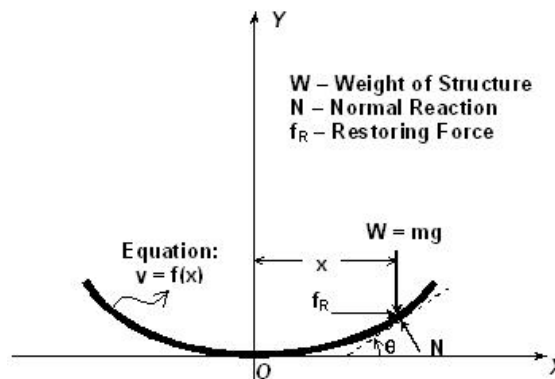


Fig. 1 Free body diagram of sliding surface

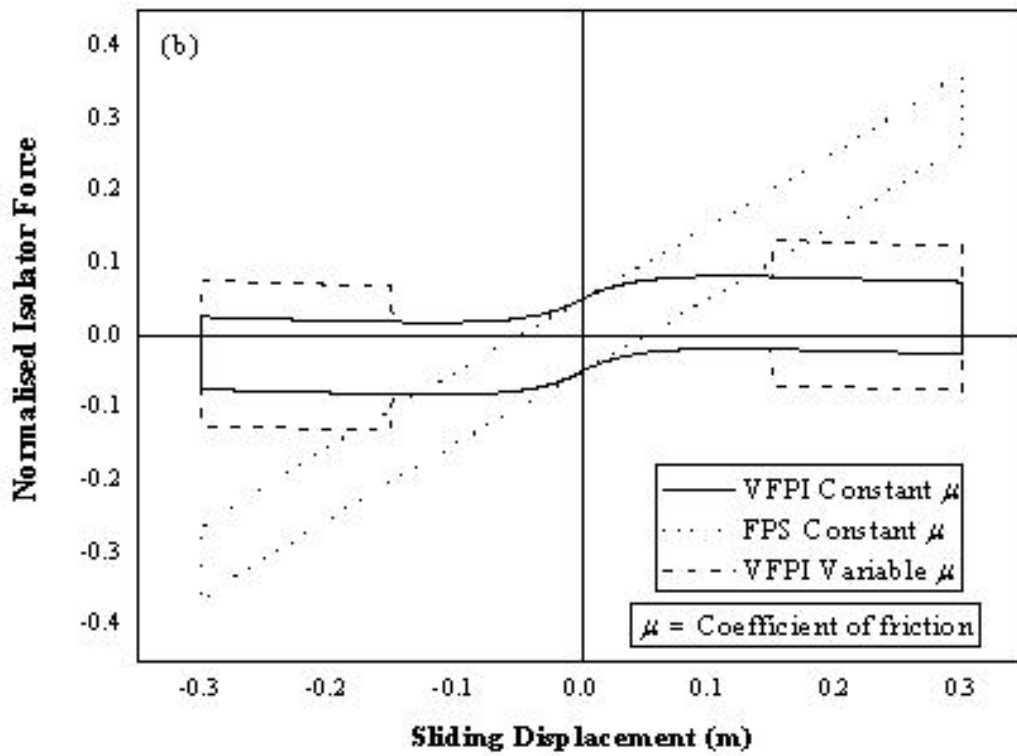
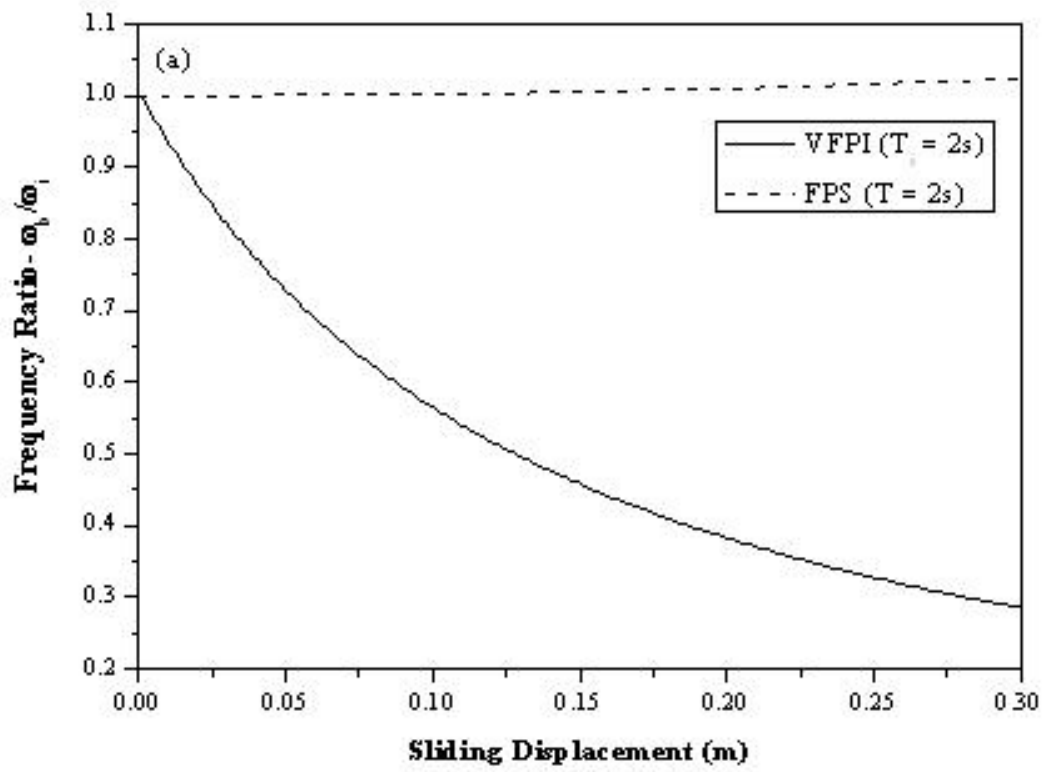


Fig. 2 Properties of VFPI and FPS (constant $\mu=0.05$, variable $\mu_1 = 0.05$, $\mu_2 = 0.1$)

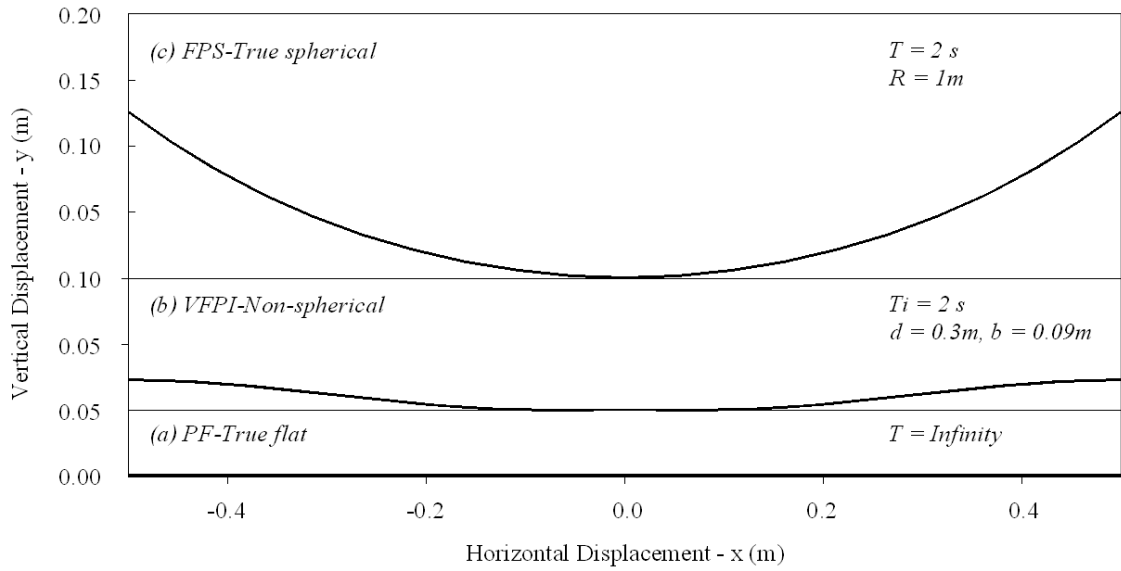


Fig. 3 Geometry of sliding surface of isolators: (a) PF (b) VFPI (c) FPS

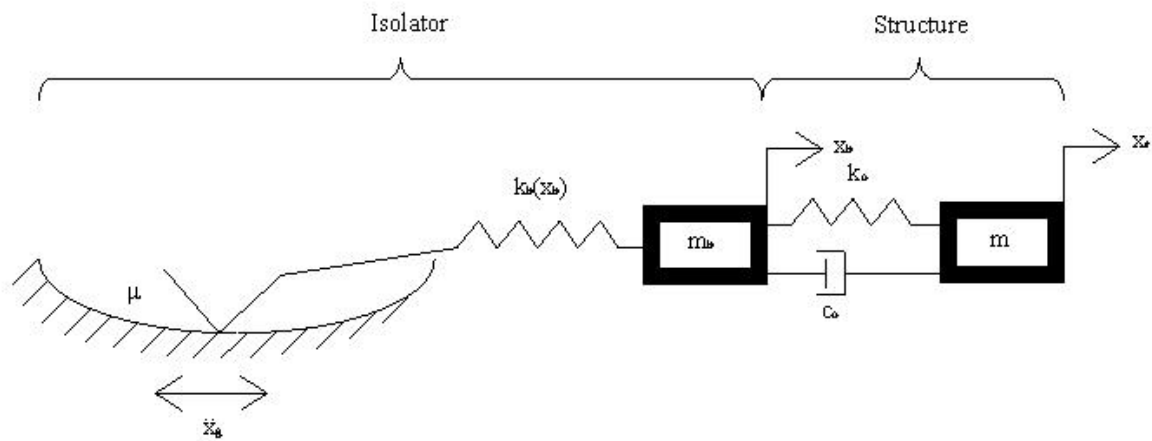


Fig. 4 Analytical model of a single storey structure isolated by curved sliding surface

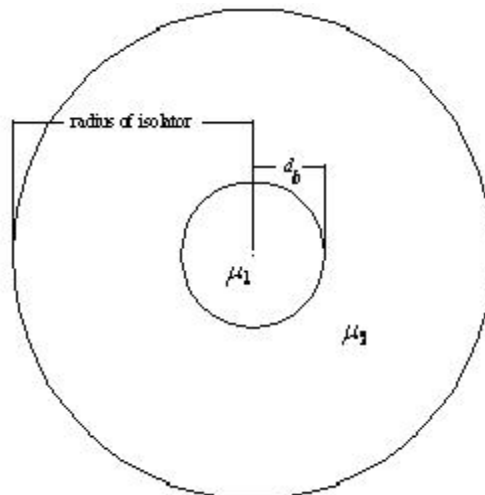


Fig. 5 Plan of typical isolator with variable coefficient of friction.

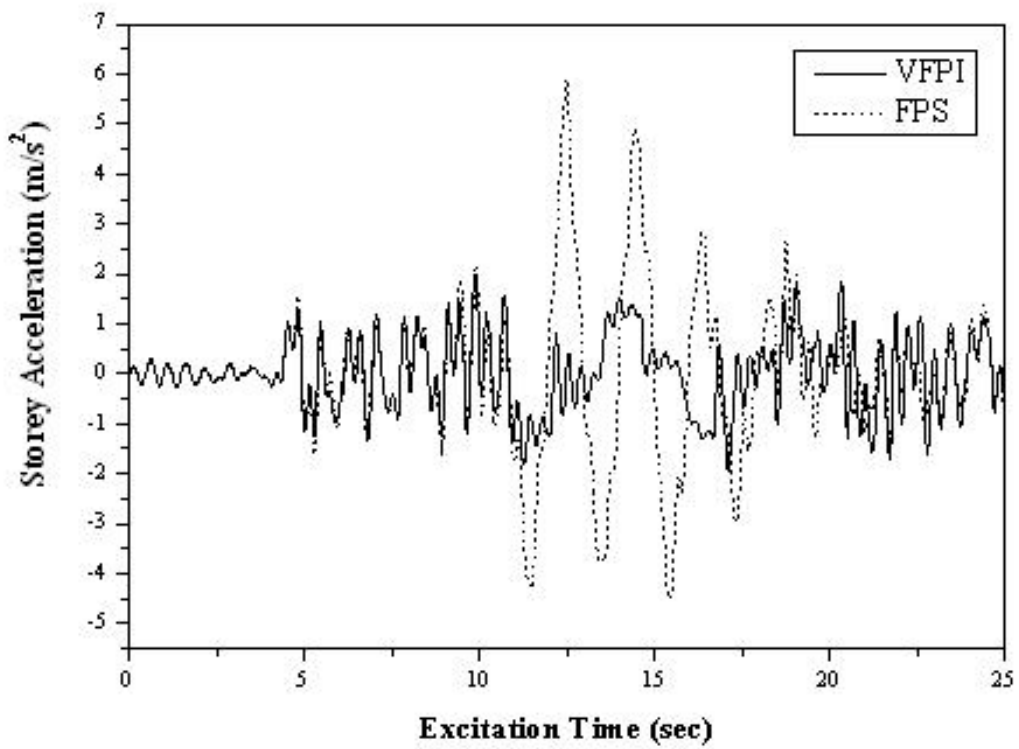


Fig. 6 Time history curve of storey acceleration for NFR-01, FVF = 2 (constant μ)

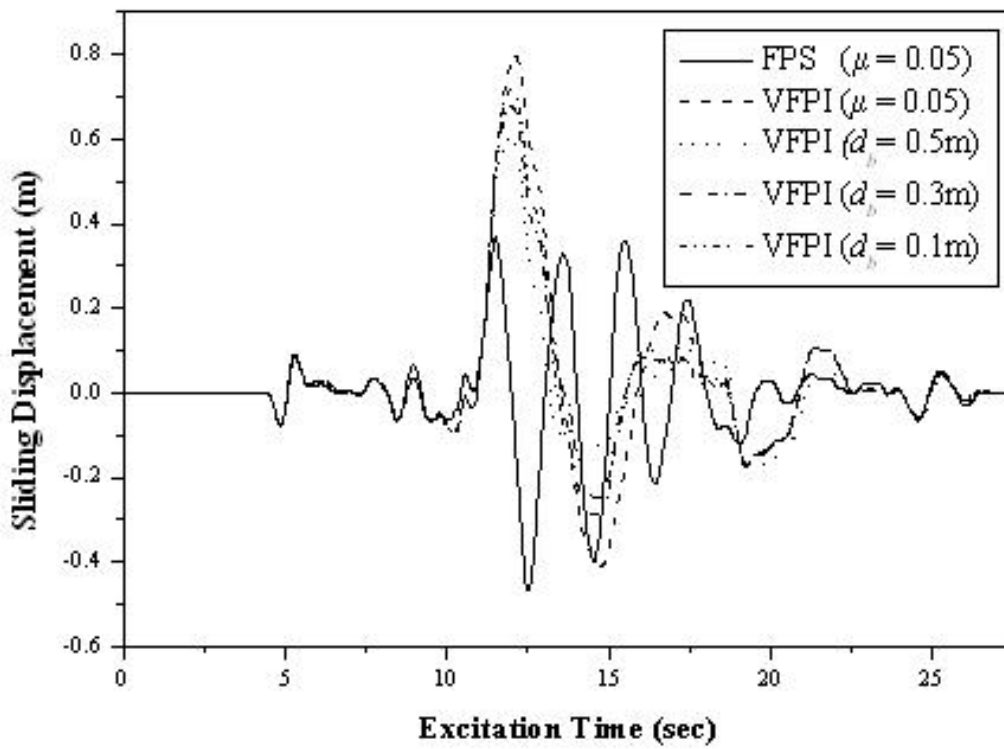


Fig. 7 Time history curve of sliding displacement for NFR-01, FVF = 2 (constant and variable μ)

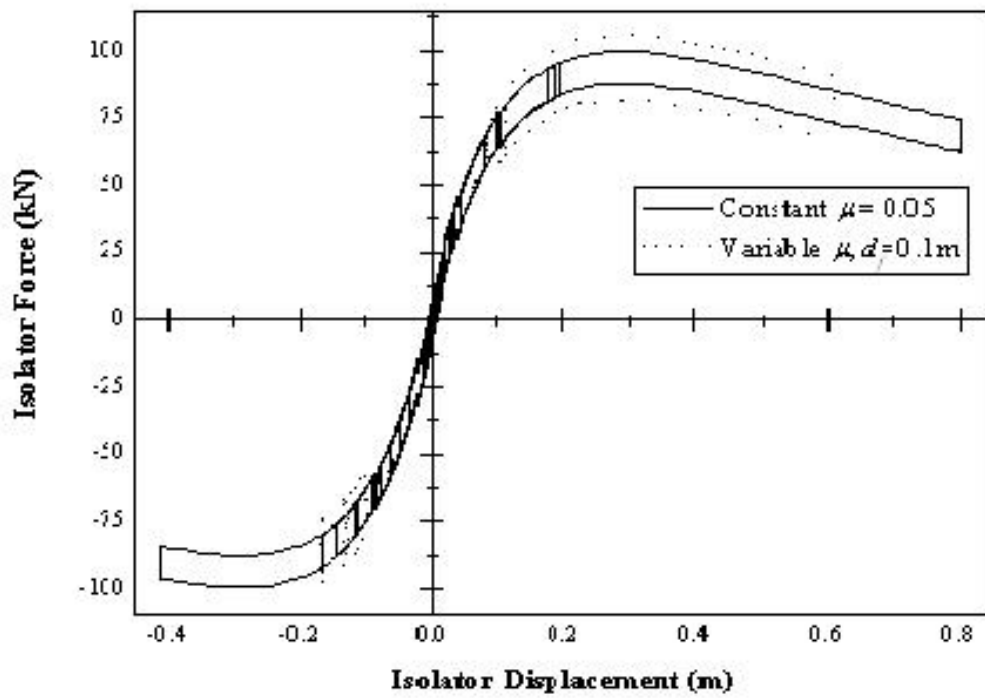


Fig. 8 Force deformation history of VFPI for constant and variable coefficient of friction for NFR-01, FVF = 2, $d_b = 0.1\text{m}$

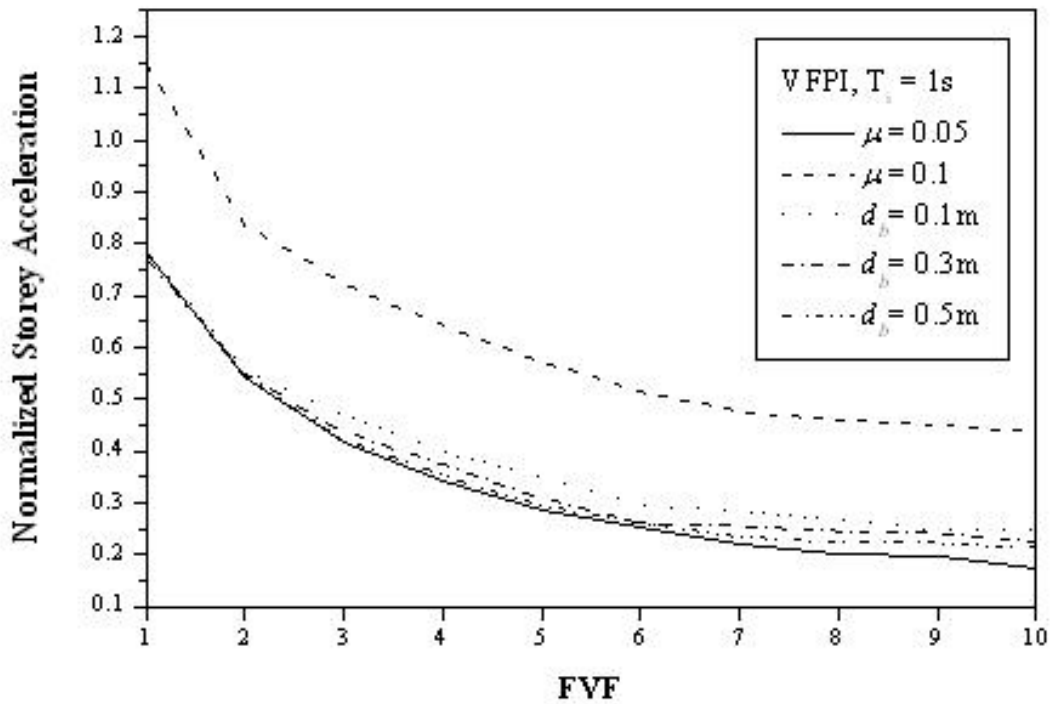


Fig. 9 Storey acceleration of VFPI ($T_i = 1\text{s}$) normalised w.r.t. peak value of FPS as in Table 2.

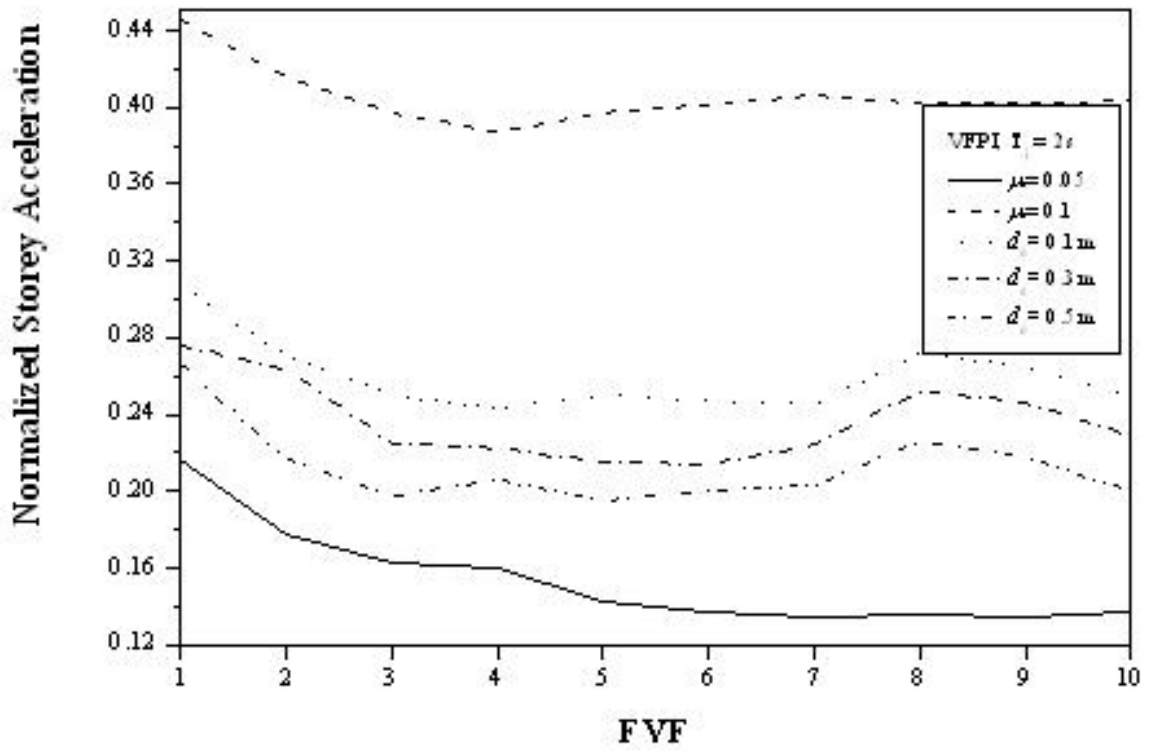


Fig. 10 Storey acceleration of VFPI ($T_i = 2s$) normalised w.r.t. peak value of FPS as in Table 2.

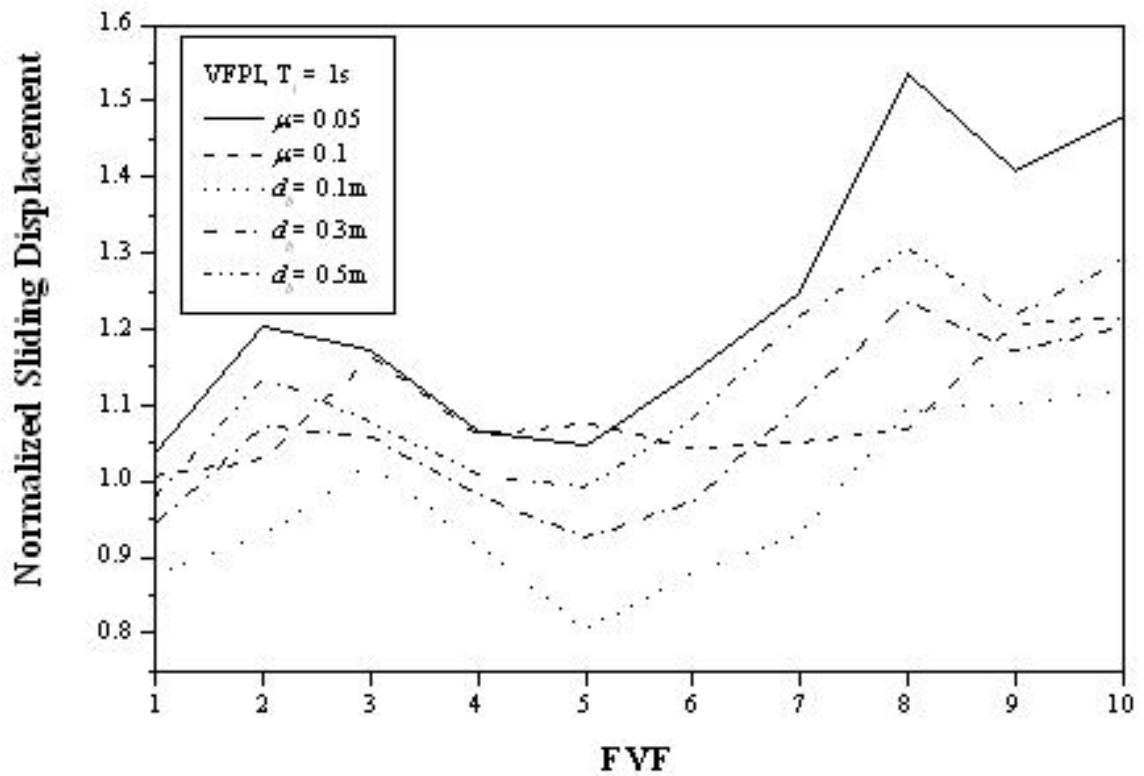


Fig. 11 Sliding displacement of VFPI ($T_i = 1s$) normalised w.r.t. peak value of FPS as in Table 2.

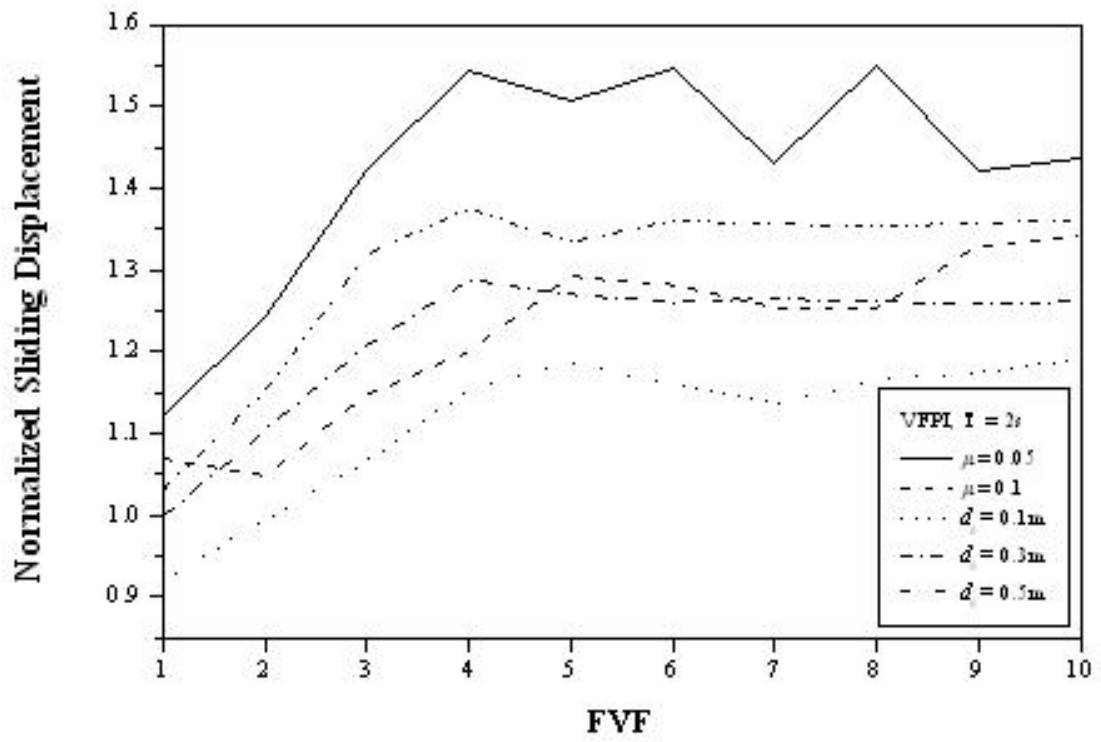


Fig. 12 Sliding displacement of VFPI ($T_i = 2s$) normalised w.r.t. peak value of FPS as in Table 2.